Energy Conversion and Management 97 (2015) 63–69

Contents lists available at ScienceDirect

Energy Conversion and Management

journal homepage: www.elsevier.com/locate/enconman

Review

Prospects for high-performance thermophotovoltaic conversion efficiencies exceeding the Shockley–Queisser limit

Zhiguang Zhou *, Qingshuang Chen, Peter Bermel

School of Electrical and Computer Engineering, Birck Nanotechnology Center, 1205 West State Street, West Lafayette, IN 47907, USA

ARTICLE INFO

Article history:
Received 25 April 2014
Accepted 11 March 2015

Keywords:
Thermophotovoltaics
Refractory metal
Selective emitter
Photonic crystal
Rugate filter
Nanophotonics

ABSTRACT

Thermophotovoltaics convert heat into electricity via thermal radiation. The efficiency of this process depends critically on the selective emitter, which can be controlled by both the choice of the material and the emitter design. We find that surveying the set of refractory and near-refractory metals yields four primary candidates: tungsten, chromium, tantalum, and molybdenum. We developed a simulation tool known as TPVtest to consider the performance of each of these candidates. Tungsten yields the highest efficiencies at 35.20% at a temperature of 1573 K. However, molybdenum comes very close to this performance at 35.12% at the same temperature. Additionally, it presents the highest efficiency of 26.15% at the same temperature for a bandgap of 1.1 eV, as found in crystalline silicon. Furthermore, it may be possible to achieve improvements beyond the efficiencies quoted here by employing composite materials and advanced photovoltaic design concepts.

Contents

1. Overview of TPV mechanism and history

Thermophotovoltaic (TPV) power systems convert heat from sources like furnaces [1] and the sun [2] into electricity via a two-step process. First, input heat generates thermal radiation at the surface of a selective emitter; second, thermal radiation is absorbed by a photovoltaic diode that converts high-energy photons into electron-hole pairs, which are subsequently captured as current [3–8].

It has recently been proposed that TPV systems can be greatly improved by modifying the selective emitters using photonic crystals (PhCs) [9] or plasmonic metamaterial structures [10–13]. Since the photon density of states and thus the thermal radiation can be strongly modified by these types of structures, one can optimize them to maximize the fraction of photons emitted at useful energies. One particular type of proposed structure uses refractory metal nanocavities with resonant modes matched to the TPV diode bandgap [14–18], which is a simpler variation on an earlier 3D photonic crystal design [19–21]. Also, selective emitters made by rare earth materials have intrinsic emission properties that may greatly improve TPV performance [22,23]. Recent work by Sakr

* Corresponding author.
E-mail address: zhou387@purdue.edu (Z. Zhou).

http://dx.doi.org/10.1016/j.enconman.2015.03.035
0196-8904/

et al. shows that ErAG emitters integrated with dielectric mirrors have theoretical TPV conversion efficiency as high as 33% [24]. Magnetic polariton-based emitters were recently proposed to achieve fixed wavelength emission at all angles, which benefits TPV systems using a fixed PV diode bandgap [25]. Refractory plasmonic structures have also been recently suggested as an alternative approach to generating spectra with similar performance [26]. Careful modeling of such designs suggests that it may even be possible to use such structures to strongly concentrate the solar spectrum into a much narrower range of photon energies. Although low-energy photons will still be emitted in all cases, a 1D photonic crystal, known as a rugate filter, can be introduced to help alleviate this problem [27]. If it is tuned to strongly reflect photons at energies below the bandgap back to the emitter, in a process known as photon recycling, the parasitic thermal losses can be greatly reduced [28–32]. This effect could also be achieved by using a strong back reflector, which is found for example in world-record GaAs cells produced by Alta Devices [33]. This form of photon recycling also complements the well-known internal photon recycling found in high-efficiency PV cells for photons at or above the bandgap energy [33]. If typical sub-bandgap and carrier thermalization losses can be strongly suppressed with this approach, extremely high heat-to-electricity power conversion efficiencies up to 50% could be achieved [7,34]. This result implies that it would also be possible to exceed the single-junction Shockley–Queisser limit for photovoltaic cells [35].

A different approach of near field TPV has also been recently proposed, which appears to have similar potential for extremely high efficiencies [36–38]. Here, a thermally-excited evanescent surface wave with a high associated local density of states is harvested by a PV diode across a sub-micron gap Δ; this additional coupling scales as Δ^{-3} [39]. In the near field regime of small Δ, thermal emission greatly exceeding the far-field blackbody limit can be achieved by exploiting surface plasmon polaritons, potentially augmented by metamaterials [40–42]. Another advantage of near field TPV is that the quasimonochromatic spectrum of near field energy transfer [43] allows high conversion efficiencies up to 40% [40]. Techniques for simulating the performance of near-field systems have also recently been developed, which could lead to new designs for even better performance [44].

These theoretical predictions have also recently seen some recent experimental validation and support. First, 2D single-crystal tungsten photonic crystals have recently been shown to give rise to thermal radiation approaching that of a blackbody at short wavelengths, while only slightly increasing thermal radiation above that of a flat metal surface at longer wavelengths [45]. Similar results have also been proven for polycrystalline tantalum photonic crystals in recent studies [46,47]. Rare earth-doped Titania nanofibers fabricated by electrospinning [48] and Er-doped YAG emitters produced by vacuum plasma-spray coating [49] have been demonstrated to have great spectral selectivity. Significant progress has also been made in the studies of TPV diodes. Silicon PV cells have been demonstrated to be suitable for certain commercial TPV applications, where costs are important and moderate power output is sufficient [50,51]. However, for most available temperature, lower bandgap materials like GaInAsSb/GaSb cells with high external quantum efficiencies are preferred, and have been successfully fabricated using organometallic vapor-phase epitaxy [52,53]. At the system level, it has been shown that 1D photonic crystal structures can be successfully integrated into millimeter-scale TPV systems, yielding higher efficiency than graybody emitter controls under equal thermal inputs, whether they be combustible fuels or solar heat [54,55]. On the other hand, high system efficiencies for converting heat into electricity, much less closely approaching the Shockley–Queisser limit, have yet to be achieved. However, there are many more possibilities to explore for these systems before the achievement of such an experimental result can be excluded.

In order to address the problem of designing such a TPV system in a realistic fashion, with its complex structures and feedback mechanisms, an analytical solution cannot be obtained, and an Edisonian approach would be prohibitively time-consuming; instead, a readily usable physics-based simulation is needed to identify key parameter regimes for further investigation. Achieving such a simulation capability also requires a suitable development and dissemination platform. NanoHUB.org, a product of Network for Computational Nanotechnology (NCN) and funded by National Science Foundation (NSF), is a science and engineering network for solving real nanotechnology problems [56]. Using an open-source development platform on nanoHUB known as Rapid Application Infrastructure (Rappture), research-quality code can be linked into a graphical user interface (GUI). That GUI can then be made widely accessible through a web-based interface without requiring users to download or compiling the codes, thus benefiting students, researchers, and educators.

In this paper, we begin by explaining the impact of photonic crystals on the components of TPV systems. First, we present the theory behind selective emitters, and why 2D arrays of holes yield much higher performance than ordinary materials. Next, we discuss how rugate filters [27,30,57] can assist in the photon recycling process. Then we develop our computational framework for evaluating the performance of the components, and linking them together logically within a system framework. We then employ this framework to evaluate a broad list of refractory and near-refractory metals, and select those with the best performance. We will then discuss additional potential improvements in both emitters and PV, with some specific suggestions for future research. Finally, we will conclude with a summary of our key findings.

2. Fundamental challenges and promise of nanoscale structuring approaches

Creating nanoscale structures can greatly impact the optical photon density of states, and would thus be expected to also strongly impact the performance of thermal radiative emitters. One example of a nanoscale structure is a photonic crystal (PhC), which is a complex dielectric structure that repeats periodically in one or more dimensions [8,9]. The most well-known characteristic of PhCs is the photonic bandgap: a range of frequencies where transmission can be strongly attenuated. Since the photovoltaic diode cannot make use of photons with energies lower than the semiconductor diode bandgap, the photonic bandgap of the

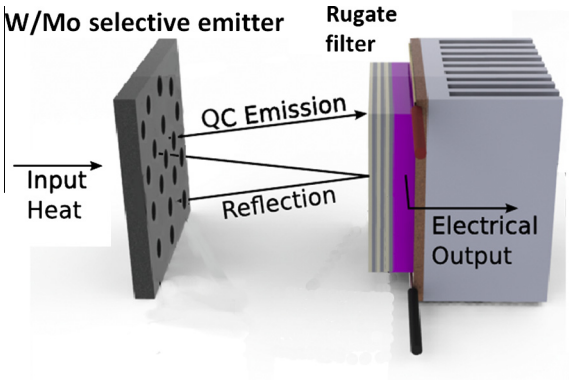

Fig. 1. A 2D tungsten or molybdenum photonic crystal or quasicrystal design is used to selectively enhance emission at shorter wavelengths to increase TPV power generation. A rugate filter is used to recycle unwanted long wavelength photons, further improving efficiency (adapted from Ref. [7]).

emitter should be chosen to match it. In Fig. 1, the basic concept of PhC-enabled conversion of heat to electricity is illustrated. In this approach, the PhC enhances selective emission at shorter wavelengths to increase the electrical output. Furthermore, a filter is introduced on the photovoltaic diode to help recycle unwanted long-wavelength photons back to the source, further improving the efficiency.

An important objective for achieving improved TPV systems is to create a selective emitter made from a 2D array of cavities in a refractory metal that allows one to achieve high optical performance with high-temperature stability. The photonic crystal emitter is designed by choosing a material with relatively high reflectivity in a planar structure, especially in the mid-infrared, and combining that with nanostructured holes. The presence of these holes allows us to engineer the rate at which photons enter the cavity, so that it can match the rate of absorption, which is known as Q-matching. This in principle can allow up to 100% emissivity at selected wavelengths. Mathematically, the Q-matching condition is given by the following equation [58]:

$$\frac{\omega_o \tau_{abs}}{2} = \frac{\omega_o \tau_{rad}}{2} = \alpha \left(\frac{d}{R}\right)^3, \quad (1)$$

where $\omega_o = 2\pi c/\lambda_o$ is the frequency, τ_{abs} and τ_{rad} are the time constants for absorption and radiation processes, d is the hole depth, R is the hole radius, and α is a constant unique to each material. The net effect of Q-matching in suitable materials is to create a strong contrast between the high emissivity regions just above the bandgap, and the low emissivity regions below. Tungsten, for example, has the correct optical properties for achieving a strong contrast between emissivities in these two regions for $\lambda_o > 1.5$ μm. However, several other materials may warrant further investigation, as will be discussed in the next section.

3. Specific material system and performance

As one of the most critical parts of the TPV system, the design of the selective emitter is carefully examined in this work. In order to have higher efficiency, higher temperatures are generally preferred. This makes refractory metals promising for selective emitter applications, because their structural integrity can be preserved even at high temperatures. On the other hand, low energy thermal photons emission increases as temperature goes up (albeit more slowly than at the higher energies dictated by Wien's law). In order to suppress low-energy photon emission, we apply a 2-D photonic crystal structure – an array of holes on the surface of the emitter – which creates a bandgap up to a cutoff frequency that can be controlled by the selection of both material and geometry.

In this work, we simulate the performance of TPV system with photonic crystal emitters made by various refractory metals by using the TPVtest simulation tool. The TPVtest tool is an integrated simulation tool we developed in order to simulate the efficiency of the TPV system as a whole. In the TPVtest tool, a finite difference time-domain (FDTD) [59] simulation developed by MIT known as MEEP [60] is employed to achieve accurate prediction of the thermal emission spectrum. The refractory metals listed above are characterized using Lorentz–Drude parameters providing the best fit to the dielectric dispersion listed in the literature [61]. A computational cell comprised of this material is then chosen to simulate a single period of the hole array, using periodic boundary conditions. A plane wave is then sent from above toward the hole array, and the reflection is calculated across a flux plane, after subtracting out the signal recorded in free space [60]. Thus, in order to properly normalize the emittance spectrum, two simulations are needed: one with, and one without, the cavity structure. This procedure thus yields the absorption spectrum. By Kirchoff's law for bodies in thermal equilibrium, the absorptivity equals the emissivity – our desired result [7]. The transmission spectrum of the rugate filter is calculated by using S4 [62]. Finally, we used the nanoHUB Rappture software development tool to combine the calculations of all the different parts into a single interface [56].

For all the different emitters, we explored a selective emitter temperature range between 573 K and 1573 K and bandgap energy between 0.2 eV and 1.4 eV. For each bandgap, we have the PV diode with its corresponding dark current density J_d, determined using the following formula:

$$J_d = J_{d0} \exp\left[(E_g - E_{g0})/kT\right], \quad (2)$$

where E_g is the bandgap, k is the Boltzmann constant, and T is the temperature of the PV diode. Following Ref. [63], we determine that $J_{d0} = 6$ μA/cm^2; $E_{g0} = 0.534$ eV, the ideality factor of the device equals 1.171, and the external quantum efficiency averages out to 0.82. The view factor (probability that emitted photons reach the receiver) is taken to be 0.99. We also chose an optimal photonic crystal emitter geometry (in terms of the period, radius and depth of the holes), and a rugate filter tuned to the chosen bandgap. For other parameters of the Rugate filter, we set the high refractive index and low refractive index as 1.91 and 1.39 respectively. And the number of bilayer periods in this work is 20.

In the remainder of this section, we will consider a set of several candidate refractory and near-refractory metals: tungsten (W), chromium (Cr), tantalum (Ta) [34], and molybdenum (Mo). In all of these, we employ the numerical model outlined above, optimized for the specific input parameters associated with each data point. Our simulations predict that two particular combinations are the most promising: a W emitter with a GaSb PV diode, and a Mo emitter with a c-Si PV diode [64]. Both have performances predicted to exceed the Shockley–Queisser limit. Furthermore, it was found that removing the rugate filters did not create too large a performance penalty to W emitter but a significant one to Mo emitter. In order to consider the contribution of the rugate filters in these two designs, we removed them while keeping all other parameters the same. The penalty for the optimal W emitter was only 1.29%, while the corresponding penalty for the optimal Mo emitter was 6.13%. In the last subsection, we will also present a table that explains why we did not perform as detailed calculations on the other refractory and near-refractory metals – due to a combination of low DC conductivities, high oxidizability/reactivity, and high costs/low earth abundance.

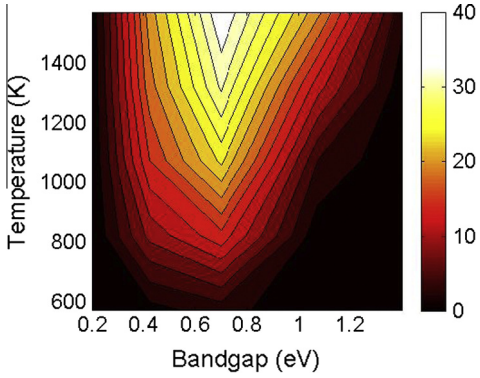

Fig. 2. Efficiency of heat-to-electricity TPV conversion of a tungsten photonic crystal selective emitter, as a function of TPV bandgap energy and temperature. The highest estimated efficiency is 35.20% when $T = 1573$ K with $E_g = 0.7$ eV. The corresponding optimized geometry is given by $a_x = a_y = 0.969$ μm; $d = 3.228$ μm; and $r = 0.397$ μm.

3.1. Tungsten

Tungsten (W) has the highest overall predicted conversion efficiency of 35.20% at 1573 K (1200 °C) The efficiency contour plot of the TPV system for a W emitter, as shown in Fig. 2, indicates that for a given bandgap energy, the efficiency increases with the temperature monotonically. However, at a fixed temperature, the efficiency first increases with the bandgap, but after a certain point it decreases, which indicates that there is an optimal value for each temperature. In general, one might expect that the optimal bandgap would increase with temperature, reflecting the blue shift of the emission spectrum associated with a higher temperature emitter. However, for W, the optimal bandgap only varies weakly with temperatures in the range from 573 K to 1573 K, centered about 0.7 eV. The physical origin of this phenomenon is that tungsten itself has a pole in one Drude–Lorentz term at 1.4 μm, which plays an important role in the emission at elevated temperatures above 1000 K [65]. Thus, for W emitters, PV diodes with E_g = 0.7 eV, like GaSb [64], are expected to provide the best performance. The highest estimated efficiency from the contour plot is 35.20% at T = 1573 K, and the corresponding geometry is given by a_x = a_y = 0.969 μm; d = 3.228 μm; r = 0.397 μm, where a_x and a_y are the period along x and y axis respectively, while d and r are the depth and radius of each hole. Furthermore, in order to consider the contribution of the rugate filters to the optimal design performance, we removed it while keeping all other parameters the same. At 1573 K, the conversion efficiency of the W emitter was 33.28%, only 1.92% less than the highest estimated efficiency.

Additionally, we may find that another metal such as chromium will serve as the hard mask for a 2-D photonic crystal selective emitter fabrication, and the residual Cr may affect the W emitter performance. Thus, we will consider Cr separately in the following section.

3.2. Chromium

The efficiency contour plot of the TPV system with a chromium (Cr) emitter given in Fig. 3 indicates that efficiency responds similarly to varying bandgap and temperature as the W emitter. But for a given temperature the best performance is lower than W, but the range of bandgaps with performance close to the maximum is very slightly wider than in W, possibly because Cr displays less sharp spectral features in the mid-infrared wavelengths [66]. This behavior is more consistent with our expectation for a blackbody-type emitter subject to Wien's law for the emission peak wavelength. For Cr, the optimal bandgap decreases when temperature goes down. The highest estimated efficiency is 28.87% when T = 1573 K and E_g = 0.7 eV, with a corresponding geometry parameterized by: a_x = a_y = 0.946 μm; d = 0.400 μm; r = 0.305 μm.

As stated above, the estimated efficiency maximum at E_g = 0.7 eV is smaller in Cr than for W (E_g = 0.7 eV). Overall, however, the spectral features are fairly similar. As a result, residual Cr may reduce the efficiency of W emitter, but only to a minor extent.

3.3. Tantalum

Tantalum has the third-highest overall conversion efficiency, after tungsten and molybdenum, but better than chromium. This reflects the fact that its DC conductivity is higher than that of Cr, which implies smaller absorption over the mid-infrared wavelengths. Such a property suppresses parasitic emission, thus allowing for a greater impact to be realized by our Q-matching approach. Much like W, the optimal bandgap is centered about 0.7 eV, and only varies with temperatures in the range from 573 K to 1573 K, as shown in Fig. 4. The physical origin of this phenomenon is that tantalum itself has a pole in one Drude–Lorentz term near 600 nm, with a full width at half maximum of approximately 300 nm [67]. Thus, for Ta emitters, PV diodes with E_g = 0.7 eV, like GaSb [64], are expected to provide the best performance. The highest estimated efficiency for Ta is 33.33% at T = 1573 K and E_g = 0.7 eV, and the corresponding geometry is: a_x = a_y = 0.969 μm; d = 6.000 μm; and r = 0.397 μm. The hole depth d is set to 6.000 μm as an upper bound, based on likely fabrication limitations.

3.4. Molybdenum

Molybdenum has the second-highest overall maximum conversion efficiency, which is consistent with its DC conductivity being higher than Ta but slightly lower than W [68]. According to the discussion above, the Q-matching approach for Mo should have more impact than in Ta, but less than in W. The efficiency predictions are shown in Fig. 5; the highest estimated efficiency is 35.12% at 1573 K for E_g = 0.7 eV. The corresponding geometry is: a_x = a_y = 0.969 μm; d = 6.000 μm; r = 0.397 μm. Just like in the case of the Tantalum emitter, aspect ratio constraints in etching are assumed to limit the hole depth d to 6.000 μm.

However, the range of bandgaps where the efficiency is close to maximum is significantly larger than for the three other materials (W, Cr, and Ta). Specifically, the highest efficiency for E_g = 1.1 eV reaches 26.15%, which also makes it a promising emitter material for TPV systems using crystalline silicon (c-Si) PV diodes [64].

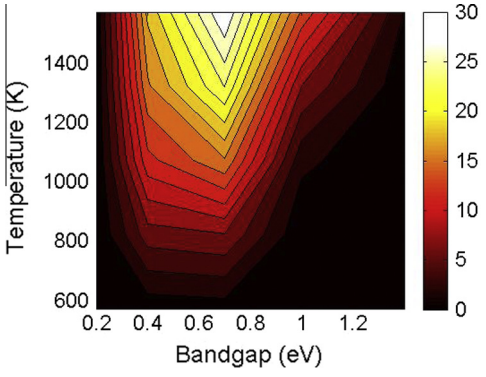

Fig. 3. Efficiency of heat-to-electricity TPV conversion of a chromium photonic crystal selective emitter, as a function of TPV bandgap energy and temperature. The highest estimated efficiency is 28.87% when T = 1573 K and E_g = 0.7 eV. The corresponding geometry is parameterized by: a_x = a_y = 0.969 μm; d = 0.400 μm; and r = 0.305 μm.

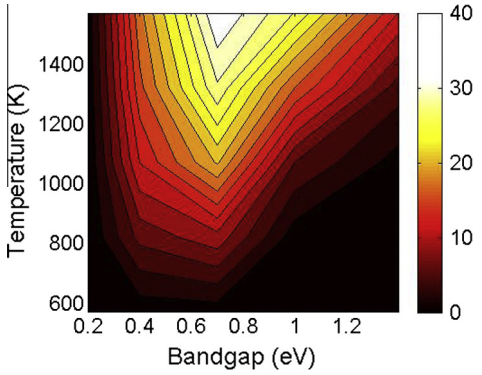

Fig. 4. Efficiency of heat-to-electricity TPV conversion of a tantalum photonic crystal selective emitter, as a function of TPV bandgap energy and temperature. The highest estimated efficiency for Ta is 33.33% when T = 1573 K and E_g = 0.7 eV, and the corresponding geometry is: a_x = a_y = 0.969 μm; d = 6.000 μm; r = 0.397 μm.

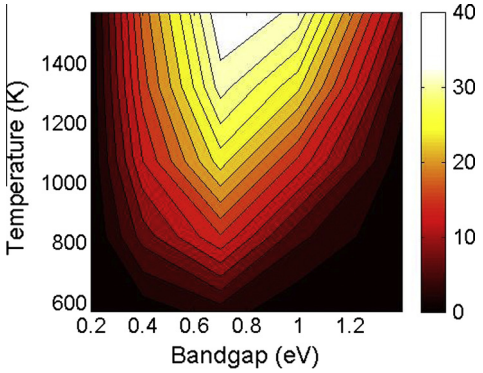

Fig. 5. Efficiency of heat-to-electricity TPV conversion of a molybdenum photonic crystal selective emitter, as a function of TPV bandgap energy and temperature. The highest estimated efficiency is 35.12% at $T = 1573$ K and $E_g = 0.7$ eV, and the corresponding geometry is: $a_x = a_y = 0.969$ μm; $d = 6.000$ μm; $r = 0.397$ μm. The highest efficiency for $E_g = 1.1$ eV reaches 26.15%, which also makes it a promising emitter material for TPV systems using c-Si PV diodes [64].

Crystalline Si PV diodes have much higher EQE compared with GaSb diodes, due to their commercial relevance, which makes the combination of Mo emitters and c-Si diodes as promising as that of W emitters and GaSb diodes.

In order to quantify the significance of the filter for the optimized Mo emitter associated with a 1.1 eV cell at 1573 K, we reran it without a filter while keeping all other parameters the same. We found that the maximum efficiency achievable would now be 20.02%, which is 6.13% less than the highest estimated efficiency. Compared to W, the Mo emitter suffers a significantly larger penalty, which shows that photon recycling is most important for large-bandgap PV diode receivers.

3.5. Other refractory metals

In choosing materials for the emitters, we must consider costs and earth abundance of key atomic constituents relative to silicon. This is because since high costs or lack of availability will sharply limit potential usefulness. Besides, one must also have a metal reflective in the infrared to ensure low parasitic emission even at high temperatures, which can be characterized by its DC conductivity. And of course, the metal itself must be stable at high temperature, which rules out mercury, indium, and the like. Metals stable at high temperature are generally referred to as refractory metals, but we also need to examine their oxidizability. In addition to W, Cr, Ta and Mo, we now consider all the other refractory metals in terms of their DC conductivities and cost-efficiency. As is listed in Table I, metals other than W, Cr, Ta and Mo are either low in DC conductivity, highly oxidizable, or extremely rare. So the investigations of W, Cr, Ta and Mo emitters performance we provide are sufficient for finding practical refractory metal emitters.

4. Future directions for research and potential performance improvements

There is a great deal of additional room for improvement for TPV systems in two major categories, which can be broadly categorized as improvements to the selective emitter (photon source), and photovoltaic diode (photon receiver).

In the selective emitter category, improvements must be concerned with decreasing parasitic losses, primarily driven by mid-infrared (mid-IR) emission that cannot be utilized. Strategies for suppressing these losses must almost necessarily take one of two forms: either choosing natural materials with lower mid-IR emissivities, or composite structures with lower mid-IR emissivities. In the former approach, future research may need to focus on finding materials combining two additional qualities: very high melting points, and at least moderate emissivity in the near-infrared or visible wavelengths. These properties may be induced by creating a tough crystalline matrix (e.g., diamond) and adding dopants and/or vacancies – for example, erbium aluminum garnet [23]. In the latter approach, advanced manmade optical structures, such as photonic crystals or metamaterials, can be utilized to induce strong reflection in the mid-infrared [10]. The advantage is that such structures could in principle be built from a wide range of materials, since the designs could be tailored for the set of available materials. Furthermore, they could also be made transparent to a highly emissive structure below in the near-IR and visible wavelengths, thus greatly relaxing the requirement for high emissivity in these regions. Another important research focus in this approach is improving the photon recycling. Photon recycling strategies using either cold-side photonic crystal filters or back reflectors are limited by the inevitable view factor between the emitter and the PV diode. Novel photon recycling strategies are needed in order to resolve the problem. Two potential solutions could be using a hot-side photonic crystal filter so that the view factor approaches unity or collimating the thermal emission via a meta-surface, so that the view factor would not automatically decline as the distance between the emitter and the PV diode is increased. For near field TPV, challenges worthy of future investigation include improved emitter-receiver alignment to achieve consistently small gap sizes without parasitic conductive losses, as well as finding appropriate resonant effects to counteract

Table I
Comparison of refractory and near-refractory metals for potential deployment as selective emitters for TPV. Desirable properties include high DC conductivity, where (a) is measured at 273 K; (b) is measured at 900 K [68], early abundance ranking [69], market cost (as of 4/4/14) [70], and oxidizability [69].

Metal name	Symbol	DC conductivity (10^8 S m^{-1})	Abundance ranking	Market cost per kg	Oxidizability
Titanium	Ti	0.026[a]	9	$6.20	High
Zirconium	Zr	0.026[a]/0.0081[b]	18	Not available	Medium
Vanadium	V	0.055[a]/0.017[b]	19	$25.50	High
Chromium	Cr	0.085[a]/0.025[b]	21	$2.09	Medium
Niobium	Nb	0.066[a]	33	Not available	Medium
Hafnium	Hf	0.033[a]	45	Not available	High
Tantalum	Ta	0.082[a]/0.025[b]	51	$153.60	Medium
Molybdenum	Mo	0.21[a]/0.047[b]	54	$23.50	Medium
Tungsten	W	0.21[a]/0.046[b]	58	$46.75	Weak
Ruthenium	Ru	0.14[a]	74	$2,539.73	Weak
Rhenium	Re	0.058[a]	77	Not available	Medium
Rhodium	Rh	0.23[a]	79	$41,094.17	Weak
Osmium	Os	0.12[a]	81	Not available	Medium
Iridium	Ir	0.21[a]	84	$20,458.91	Weak

the unfavorable effects of spectrum broadening and increased dark current in PV diode [38,71].

Regarding the category of improvements to the photovoltaic diode – one could in principle utilize one or more of the many approaches currently under investigation in the photovoltaic literature already, which include multijunction cells, quantum well cells [72,73], spectral splitting, multiple exciton generation, hot carrier cells, and intermediate bandgap cells [74]. Of these, to date, only multijunction cells and spectral splitting have been experimentally shown to exceed the Shockley–Queisser limit [75]. However, it should be noted that converting low-energy photons becomes increasingly difficult at lower emitter temperatures, due to thermal losses, so the incremental advantage of multiple junctions or spectrally split bins is lower than in the photovoltaic case. In a potentially more fruitful direction, recent developments in epitaxial liftoff films, used to enable record open-circuit voltages and conversion efficiencies in gallium arsenide (GaAs) [76], could also be applied to smaller-bandgap III–V materials, such as gallium antimonide (GaSb) [64].

Future studies need to consider combining the two major approaches outlined above. For example, it might be of great interest to develop a quasicrystal with rotational symmetry exceeding that of a square lattice in order to maximize isotropic emission and decrease losses, while on the diode side, to develop epitaxial liftoff processes for smaller-bandgap III–V materials to achieve high performance in the presence of both internal and external photon recycling.

5. Summary and conclusions

In conclusion, we examined a broad set of refractory and near-refractory metals as candidates for selective emitters in thermophotovoltaic (TPV) systems. The need for materials with high melting points, low mid-infrared emissivity, and reasonable earth abundance led us to four candidates: tungsten (W), chromium (Cr), tantalum (Ta), and molybdenum (Mo). A contour plot of conversion efficiencies as a function of bandgap and temperature was generated for each material. Maximum efficiencies found on the contour plots are provided with detailed parameters that can be used as references for the broad applications of photonic crystals in TPV research. Out of these materials, we found that tungsten was the best overall performer, with potential heat-to-electricity conversion efficiencies up to 35.20%. However, molybdenum was close behind, with efficiencies up to 35.12%; furthermore, we found that it was capable of efficiencies up to 26.15% at bandgaps of 1.1 eV, which would make it compatible with silicon photovoltaic diodes already widely produced with high performance at low cost. It also implies the potential applications of larger bandgap PV diodes in high performance TPV systems. Thus, both tungsten and molybdenum have the potential to exceed the Shockley–Queisser limit for converting concentrated sunlight into electricity. Further improvements beyond the efficiencies quoted here may also be possible if we utilize greater sophistication in the design of the selective emitters or photovoltaic diodes employed in the conversion process by incorporating key concepts such as photon recycling.

Acknowledgments

We thank Roman Shugayev, Enas Sakr, Urcan Guler, and Vlad Shalaev for valuable discussions. This work was supported by the U.S. National Science Foundation through grant EEC-0634750 (Network for Computational Nanotechnology) and the Semiconductor Research Corporation through TERC Contract 2010-ER-2110 (Network for Photovoltaic Technology).

References

[1] Fraas LM, Avery JE, Huang HX. Thermophotovoltaics: heat and electric power from low bandgap "solar" cells around gas fired radiant tube burners. In: Conf rec twenty-ninth IEEE photovolt spec conf 2002; 2002.
[2] Davies PA, Luque A. Solar thermophotovoltaics – brief review and a new look. Sol Energy Mater Sol Cells 1994;33:11–22.
[3] Bauer T. Thermophotovoltaics: basic principles and critical aspects of system design. Springer Science & Business Media; 2011.
[4] Coutts TJ, Wanlass MW, Ward JS, Johnson S. A review of recent advances in thermophotovoltaics. In: Conf rec twenty fifth IEEE photovolt spec conf – 1996; 1996.
[5] Kholm H. Solar-battery power source. Q. Prog. Rep. 1956:13.
[6] Chubb D. Fundamentals of thermophotovoltaic energy conversion. Elsevier; 2007.
[7] Bermel P, Ghebrebrhan M, Chan W, Yeng YX, Araghchini M, Hamam R, et al. Design and global optimization of high-efficiency thermophotovoltaic systems. Opt Express 2010;18(Suppl 3):A314–34.
[8] Celanovic I, Bermel P, Soljacic M. Thermophotovoltaic power conversion systems : current performance and future potential. Invit Rev Artic Oyo Buturi (Jpn Soc Appl Phys) 2011.
[9] Joannopoulos JD, Johnson S, Winn JNJ, Meade RRD. Photonic crystals: molding the flow of light; 2008.
[10] Maier SA. Plasmonics: fundamentals and applications. Springer Science & Business Media; 2007.
[11] Cai W, Shalaev V. Optical metamaterials: fundamentals and applications; 2010.
[12] Wu C, Neuner BI, John J, Milder A, Zollars B, Savoy S, et al. Metamaterial-based integrated plasmonic absorber/emitter for solar thermo-photovoltaic systems. J Opt 2012;14:024005.
[13] Molesky S, Dewalt CJ, Jacob Z. High temperature epsilon-near-zero and epsilon-near-pole metamaterial emitters for thermophotovoltaics. Opt Express 2013;21(Suppl 1):A96–A110.
[14] Sai H, Kanamori Y, Yugami H. High-temperature resistive surface grating for spectral control of thermal radiation. Appl Phys Lett 2003;82:1685–7.
[15] Sai H, Yugami H. Thermophotovoltaic generation with selective radiators based on tungsten surface gratings. Appl Phys Lett 2004;85:3399–401.
[16] Celanovic I, Perreault D, Kassakian J. Resonant-cavity enhanced thermal emission. Phys Rev B 2005;72:2–7.
[17] Chan DLC, Celanovic I, Joannopoulos JD, Soljačić M. Emulating one-dimensional resonant Q -matching behavior in a two-dimensional system via Fano resonances. Phys Rev A – At Mol Opt Phys 2006;74:1–4.
[18] Celanovic I, Jovanovic N, Kassakian J. Two-dimensional tungsten photonic crystals as selective thermal emitters. Appl Phys Lett 2008;92:1–3.
[19] John S, Wang R. Metallic photonic-band-gap filament architectures for optimized incandescent lighting. Phys Rev A – At Mol Opt Phys 2008;78:1–10.
[20] Gee JM, Moreno JB, Lin S, Fleming JG. Selective emllters using photonic crystals for thermophotovoltaic energy conversion. In: Conf rec twenty-ninth IEEE photovolt spec conf; 2002. p. 896–9.
[21] Florescu M, Lee H, Puscasu I, Pralle M, Florescu LZ, Ting D, et al. Improving solar cell efficiency using photonic band-gap materials. Sol Energy Mater Sol Cells 2007;91:1599–610.
[22] Bitnar B, Durisch W, Mayor JC, Sigg H, Tschudi HR. Characterisation of rare earth selective emitters for thermophotovoltaic applications. Sol Energy Mater Sol Cells 2002;73:221–34.
[23] Chubb DL, Pal AT, Patton MO, Jenkins PP. Rare earth doped high temperature ceramic selective emitters. J Eur Ceram Soc 1999;19:2551–62.
[24] Sakr ES, Zhou Z, Bermel P. High efficiency rare-earth emitter for thermophotovoltaic applications. Appl Phys Lett 2014;105:111107.
[25] Wang LP, Zhang ZM. Wavelength-selective and diffuse emitter enhanced by magnetic polaritons for thermophotovoltaics. Appl Phys Lett 2012:100.
[26] Guler U, Boltasseva A, Shalaev VM. Refractory plasmonics. Science 2014;344:263–4 (80-).
[27] Bovard BG. Rugate filter theory: an overview. Appl Opt 1993;32:5427–42.
[28] Black R., Martin L, Baldasaro PF. Thermophotovoltaics-development status and parametric considerations for power applications. In: Thermoelectr 1999. Eighteenth int conf; 1999. p. 639–44.
[29] Heinzel A, Boerner V, Gombert A, Blasi B, Wittwer V, Luther J. Radiation filters and emitters for the NIR based on periodically structured metal surfaces. J Mod Opt 2000;47:2399–419.
[30] Ortabasi U. Rugate technology for thermophotovoltaic (TPV) applications: a new approach to near perfect filter performance. In: Fifth conf thermophotovoltaic gener electr, vol. 653; 2003. p. 249–58.
[31] O'Sullivan F, Celanovic I, Jovanovic N, Kassakian J, Akiyama S, Wada K. Optical characteristics of one-dimensional Si/SiO_2 photonic crystals for thermophotovoltaic applications. J Appl Phys 2005;97:033529.
[32] Rahmlow Jr TD, DePoy DM, Fourspring PM, Ehsani H, Lazo-Wasem JE, Gratrix EJ. Development of front surface, spectral control filters with greater temperature stability for thermophotovoltaic energy conversion. In: Thermophotovoltaic gener electr TPV7 seventh world conf thermophotovoltaic gener electr. AIP Publishing; 2007. p. 59–67.
[33] Miller OD, Yablonovitch E. Photon extraction: the key physics for approaching solar cell efficiency limits. SPIE Act Photonics V; 2013.
[34] Nam Y, Yeng YX, Lenert A, Bermel P, Celanovic I, Soljačić M, et al. Solar thermophotovoltaic energy conversion systems with two-dimensional

tantalum photonic crystal absorbers and emitters. Sol Energy Mater Sol Cells 2014;122:287–96.
[35] Shockley W, Queisser HJ. Detailed balance limit of efficiency of p–n junction solar cells. J Appl Phys 1961;32:510–9.
[36] Narayanaswamy A, Chen G. Surface modes for near field thermophotovoltaics. Appl Phys Lett 2003;82:3544–6.
[37] DiMatteo RS, Greiff P, Finberg SL, Young-Waithe KA, Choy HKH, Masaki MM, et al. Micron-gap thermophotovoltaics (MTPV). AIP Conf Proc 2003; 653:232–40.
[38] Laroche M, Carminati R, Greffet JJ. Near-field thermophotovoltaic energy conversion. J Appl Phys 2006:100.
[39] Petersen SJ, Basu S, Francoeur M. Near-field thermal emission from metamaterials. Photonics Nanostruct – Fundam Appl 2013;11:167–81.
[40] Ilic O, Jablan M, Joannopoulos JD, Celanovic I, Soljačić M. Overcoming the black body limit in plasmonic and graphene near-field thermophotovoltaic systems. Opt Express 2012;20:A366.
[41] Biehs SA, Tschikin M, Messina R, Ben-Abdallah P. Super-Planckian near-field thermal emission with phonon-polaritonic hyperbolic metamaterials. Appl Phys Lett 2013:102.
[42] Guo Y, Cortes CL, Molesky S, Jacob Z. Broadband super-Planckian thermal emission from hyperbolic metamaterials. Appl Phys Lett 2012:101.
[43] Mulet J-P, Joulain K, Carminati R, Greffet JJ. Enhanced radiative heat transfer at nanometer distances. Microscale Thermophys Eng 2002;6:209–22.
[44] Rodriguez AW, Ilic O, Bermel P, Celanovic I, Joannopoulos JD, Soljačić M, et al. Frequency-selective near-field radiative heat transfer between photonic crystal slabs: a computational approach for arbitrary geometries and materials. Phys Rev Lett 2011:107.
[45] Yeng YX, Ghebrebrhan M, Bermel P, Chan WR, Joannopoulos JD, Soljacic M, et al. Enabling high-temperature nanophotonics for energy applications. Proc Natl Acad Sci 2012;109:2280–5.
[46] Rinnerbauer V, Ndao S, Yeng YX, Chan WR, Senkevich JJ, Joannopoulos JD, et al. Recent developments in high-temperature photonic crystals for energy conversion. Energy Environ Sci 2012;5:8815.
[47] Rinnerbauer V, Yeng YX, Chan WR, Senkevich JJ, Joannopoulos JD, Soljačić M, et al. High-temperature stability and selective thermal emission of polycrystalline tantalum photonic crystals. Opt Express 2013;21:11482–91.
[48] Tomer V, Teye-Mensah R, Tokash JC, Stojilovic N, Kataphinan W, Evans EA, et al. Selective emitters for thermophotovoltaics: erbia-modified electrospun titania nanofibers. Sol Energy Mater Sol Cells 2005;85:477–88.
[49] Tobler WJ, Durisch W. High-performance selective Er-doped YAG emitters for thermophotovoltaics. Appl Energy 2008;85:483–93.
[50] Bitnar B. Silicon, germanium and silicon/germanium photocells for thermophotovoltaics applications. Semicond Sci Technol 2003;18:S221–7.
[51] Qiu K, Hayden ACS. Development of a silicon concentrator solar cell based TPV power system. Energy Convers Manage 2006;47:365–76.
[52] Wang CA, Choi HK, Oakley DC, Charache GW. Recent progress in GaInAsSb thermophotovoltaics grown by organometallic vapor-phase epitaxy. J Cryst Growth 1998;195:346–55.
[53] Wang CA, Choi HK, Ransom SL, Charache GW, Danielson LR, DePoy DM. High-quantum-efficiency 0.5 eV GaInAsSb/GaSb thermophotovoltaic devices. Appl Phys Lett 1999;75:1305.
[54] Chan WR, Bermel P, Pilawa-Podgurski RCN, Marton CH, Jensen KF, Senkevich JJ, et al. Toward high-energy-density, high-efficiency, and moderate-temperature chip-scale thermophotovoltaics. Proc Natl Acad Sci 2013;110:5309–14.
[55] Lenert A, Bierman DM, Nam Y, Chan WR, Celanović I, Soljačić M, et al. A nanophotonic solar thermophotovoltaic device. Nat Nanotechnol 2014;9:1–5.
[56] Klimeck G, Mclennan M, Brophy SB, Adams GB, Lundstrom MS. NanoHUBorg: advancing education and research in nanotechnology. Comput Sci Eng 2008;10:17–23.
[57] Carniglia CK. Comparison of several shortwave pass filter designs. Appl Opt 1989;28:2820–3.
[58] Ghebrebrhan M, Bermel P, Yeng YX, Celanovic I, Soljačić M, Joannopoulos JD. Tailoring thermal emission via Q matching of photonic crystal resonances. Phys Rev A - At Mol Opt Phys 2011;83:1–6.
[59] Taflove A, Hagness SC. Computational electrodynamics: the finite-difference time-domain method. Artech House; 2000.
[60] Oskooi AF, Roundy D, Ibanescu M, Bermel P, Joannopoulos JD, Johnson SG. Meep: a flexible free-software package for electromagnetic simulations by the FDTD method. Comput Phys Commun 2010;181:687–702.
[61] Palik ED. Handbook of optical constants of solids, vol. 3. Academic Press/ Elsevier; 1998.
[62] Liu V, Fan S. S 4: a free electromagnetic solver for layered periodic structures. Comput Phys Commun 2012;183:2233–44.
[63] Chan W, Huang R, Wang C, Kassakian J, Joannopoulos J, Celanovic I. Modeling low-bandgap thermophotovoltaic diodes for high-efficiency portable power generators. Sol Energy Mater Sol Cells 2010;94:509–14.
[64] Kittel C, McEuen P. Introduction to solid state physics. 8th ed. John Wiley and Sons; 1976.
[65] Roberts S. Optical properties of nickel and tungsten and their interpretation according to drude's formula. Phys Rev 1959;114:104–15.
[66] Rakic AD, Djurisic AB, Elazar JM, Majewski ML. Optical properties of metallic films for vertical-cavity optoelectronic devices. Appl Opt 1998;37:5271–83.
[67] Nestell JE, Christy RW. Optical conductivity of bcc transition metals: V, Nb, Ta, Cr, Mo, W. Phys Rev B 1980;21:3173–9.
[68] Lide DR. CRC handbook of chemistry and physics, 94th ed., vol. 53, 2013–2014; 2013.
[69] Emsley J. Nature's building blocks: an A–Z guide to the elements. Oxford University Press; 2011.
[70] Robinson A, Baldwin G. Infomine, incorporated worldwide mining information service; 2014, <http://www.infomine.com/investment/metal-prices/> [accessed 4.04.14].
[71] Baldasaro PF, Raynolds JE, Charache GW, DePoy DM, Ballinger CT, Donovan T, et al. Thermodynamic analysis of thermophotovoltaic efficiency and power density tradeoffs. J Appl Phys 2001;89:3319–27.
[72] Griffin P, Ballard I, Barnham K, Nelson J, Zachariou A, Epler J, et al. The application of quantum well solar cells to thermophotovoltaics. Sol Energy Mater Sol Cells 1998;50:213–9.
[73] Connolly JP, Rohr C. Quantum well cells for thermophotovoltaics. Semicond Sci Technol 2003;18:S216–20.
[74] Green MA. Third generation photovoltaics: ultra-high conversion efficiency at low cost. Prog Photovoltaics Res Appl 2001;9:123–35.
[75] Imenes AG, Mills DR. Spectral beam splitting technology for increased conversion efficiency in solar concentrating systems: a review. Sol Energy Mater Sol Cells 2004;84:19–69.
[76] Green MA, Emery K, Hishikawa Y, Warta W, Dunlop ED. Solar cell efficiency tables (version 42). Prog Photovoltaics Res Appl 2013;21:827–37.